MICROBIOLOGY

RESEARCH ARTICLE

Jacob *et al.*, *Microbiology* 2017;163:541–553

DOI 10.1099/mic.0.000396

# Unravelling the biosynthesis of pyriculol in the rice blast fungus *Magnaporthe oryzae*

Stefan Jacob,[1,*] Thomas Grötsch,[1] Andrew J. Foster,[1] Anja Schüffler,[1] Patrick H. Rieger,[1] Louis P. Sandjo,[2] Johannes C. Liermann,[2] Till Opatz[2] and Eckhard Thines[1,3,*]

**Abstract**

Pyriculol was isolated from the rice blast fungus *Magnaporthe oryzae* and found to induce lesion formation on rice leaves. These findings suggest that it could be involved in virulence. The gene *MoPKS19* was identified to encode a polyketide synthase essential for the production of the polyketide pyriculol in the rice blast fungus *M. oryzae*. The transcript abundance of *MoPKS19* correlates with the biosynthesis rate of pyriculol in a time-dependent manner. Furthermore, gene inactivation of *MoPKS19* resulted in a mutant unable to produce pyriculol, pyriculariol and their dihydro derivatives. Inactivation of a putative oxidase-encoding gene *MoC19OXR1*, which was found to be located in the genome close to *MoPKS19*, resulted in a mutant exclusively producing dihydropyriculol and dihydropyriculariol. By contrast, overexpression of *MoC19OXR1* resulted in a mutant strain only producing pyriculol. The *MoPKS19* cluster, furthermore, comprises two transcription factors *MoC19TRF1* and *MoC19TRF2*, which were both found individually to act as negative regulators repressing gene expression of *MoPKS19*. Additionally, extracts of Δ*Mopks19* and Δ*MoC19oxr1* made from axenic cultures failed to induce lesions on rice leaves compared to extracts of the wild-type strain. Consequently, pyriculol and its isomer pyriculariol appear to be the only lesion-inducing secondary metabolites produced by *M. oryzae* wild-type (*Mo*WT) under these culture conditions. Interestingly, the mutants unable to produce pyriculol and pyriculariol were as pathogenic as *Mo*WT, demonstrating that pyriculol is not required for infection.

## INTRODUCTION

Fungal secondary metabolites play crucial roles in plant–pathogen interactions and it appears to be of particular interest to elucidate their function in respect of the biological activity and the organization of their biosynthetic pathways. Fungal pathogens, especially hemibiotrophic specimens, initially establish a biotrophic relationship with their host and and are supposed to produce toxic secondary metabolites mostly during late infection [1]. *Magnaporthe oryzae* causes rice blast disease and is one of the most significant plant pathogens worldwide [2]. This filamentous ascomycete has been studied intensively and has become an excellent model organism for studying the molecular mechanisms of plant–pathogen interaction. In contrast to infection-related morphogenesis *ex planta* [3, 4], which has been investigated intensively, little is known about invasive growth, metabolic adjustments and microbe–host interaction during the colonization *in planta*. One of the fungal secondary metabolites studied most intensively is the polyketide dihydroxynaphthalene (DHN) melanin. Melanin is a dark brown pigment accumulating in fungal cell walls, thereby protecting the mycelium and conidia against desiccation, reactive oxygen species and UV light [5]. DHN melanin was found to be essential in *M. oryzae* for appressorium function and, thereby, for pathogenic development. DHN-melanin is required for the generation of an enormous turgor within the appressorium needed for host penetration [6]. The biosynthetic pathway of DHN was investigated by using melanin-deficient mutant strains, and the main biosynthetic intermediates were uncovered [5]. Further secondary metabolites involved in the virulence of the rice blast fungus were believed to be produced by the polyketide synthase [PKS-nonribosomal peptide synthase (NRPS)] MoAce1p. The gene *MoACE1* encodes an intracellular hybrid protein which was found to be involved in effects concerning the rice resistance gene *Pi33* [7, 8].

Received 8 August 2016; Accepted 16 November 2016

**Author affiliations:** [1]Institut für Biotechnologie und Wirkstoff-Forschung gGmbH (IBWF), Erwin-Schrödinger Str. 56, D-67663 Kaiserslautern, Germany; [2]Institute of Organic Chemistry, Johannes Gutenberg University of Mainz, Duesbergweg 10-14, D-55128 Mainz, Germany; [3]Institut für Mikrobiologie und Weinforschung, Johannes Gutenberg University of Mainz, Johann-Joachim-Becherweg 15, D-55128 Mainz, Germany.
***Correspondence:** Stefan Jacob, jacob@ibwf.de; Eckhard Thines, thines@ibwf.de

**Keywords:** pyriculol; phytotoxin; *Magnaporthe oryzae*; secondary metabolite; PKS gene cluster; secondary metabolite biosynthesis; gene cluster regulation; virulence; polyketide synthases; plant–microbe interaction.

**Abbreviations:** DHN, dihydroxynaphthalene; PKS, polyketide synthase; qRT-PCR, quantitative real-time PCR.

Four supplementary figures and three supplementary tables are available with the online Supplementary Material

Species of the rice blast fungus were found to produce a variety of phytotoxic secondary metabolites dependent on the way it was cultivated *in vitro*. For example, *Magnaporthe grisea* was found to produce a species-specific metabolite, pyrichalasin [9, 10]. The virulence of the *Digitaria*-pathogenic *M. grisea* strains putatively correlates with the quantity of pyrichalasin H because toxin-free mutants were non-pathogenic – but a comprehensive characterization of these mutants has not been not conducted to date [11]. Additional studies have identified other metabolites produced by *Magnaporthe* strains, i.e. tenuazonic acid and Magtoxin [10, 12–14]. Tenuazonic acid is a mycotoxin synthesized by various plant pathogenic fungi. The biosynthesis was hypothesized in *M. oryzae*from isoleucine and acetoacetyl-CoA by TeA synthetase 1 (*TAS1*) [14]. Furthermore, metabolome studies resulted in varieties of metabolites, i.e. siderophores found to be essential for host invasion. One of them is ferricrocin which was suggested to play a role in pathogenicity since mutants unable to produce ferricrocin were reduced in virulence [15]. Furthermore, it was hypothesized that the loss of an Abc3 pump leads to excessive accumulation of its physiological substrate, a digoxin-like endogenous steroidal glycoside, to likely inhibitory levels resulting in appressorial dysfunction [16]. The many common patterns of metabolomic re-programming during *in planta* growth was described in pre-symptomatic tissues, proliferation and hyphal growth of *M. oryzae,* indicating that that fungal pathogens deploy a common metabolic re-programming strategy in diverse host species to suppress plant defence and colonize plant tissue. Metabolization of monosaccharides into mannitol and glycerol for carbon sequestration and osmolyte production was suggested to drive hyphal growth *in planta* [17]. Furthermore, a series of salicylaldehyde-type phytotoxins, such as pyriculol and pyriculariol, were found and putative biosynthetic intermediates of these compounds were synthesized to elucidate the biosynthesis [18]. However, no further studies have been published to date concerning the *M. oryzae* PKS gene cluster with respect to the biosynthesis of pyriculol and pyriculariol. We identified the *PKS19* gene cluster within this study and present the four genes *MoPKS19*, *MoC19OXR1*, *MoC19TRF1* and *MoC19TRF2* contributing to the regulation of the biosynthesis of pyriculol and pyriculariol. Furthermore, both compounds were found to be dispensable for pathogenicity in the rice blast fungus, since mutants unable to synthesize the heptaketides were found to be as virulent as the wild-type strain.

## METHODS

### Strains, culture/growth conditions and oligonucleotides

All mutants described in this study were generated from *M. oryzae* (*M. oryzae* 70-15 strain: *Mo*WT, Fungal Genetics Stock Centre, Kansas City, USA). The strains were grown at 26 °C on complete medium (CM) [19]. All oligonucleotides used in this study are listed in Table S1 (available in the online Supplementary Material) and were obtained from Eurofins MWG Operon. All chemicals used were of p.a. (pro analysis) quality unless otherwise stated.

### Identification and sequence analysis of polyketide synthase genes in *M. oryzae*

Sequence analysis and comparison of the PKS-related genes in the *M. oryzae* genome [*Magnaporthe* Comparative Sequencing Project, Broad Institute of Harvard and MIT (www.broadinstitute.org/); MG8] were performed by the Basic Local Alignment Search Tool (BLAST; http://genome.jgi.doe.gov/pages/blast-query.jsf?db=Maggr1). Protein domains and further information were obtained from the InterProScan database (www.ebi.ac.uk/Tools/pfa/iprscan).

### DNA manipulation/construction of gene deletion/expression vectors

The DNA of *Mo*WT was isolated from mycelia of 3-day-old liquid cultures (grown in CM at 26 °C and 120 r.p.m.) using a DNeasy Plant Mini kit (QIAGEN) following the manufacturer's instructions for purification of DNA from plants and filamentous fungi. Standard procedures were carried out for DNA manipulation [20].

Fungal transformations were conducted using *Agrobacterium tumefaciens*-mediated transformation, as described in previous studies [21, 22]. Mutant strains were generated using hygromycin resistance to interrupt and respectively replace parts of the coding sequences of the target genes. By contrast, the complementation of mutant strains was conducted using the *ILV* gene mediating resistance to chlorimuron ethyl [23]. See supplementary material S1 for detailed information on the deletion/expression strategies.

### Phylogenetic tree of MoPks19p and sequence analysis

Phylogenetic analysis was carried by using the program MEGA 5.2 [24]. Sequence alignments were performed using CLUSTALW [25]. BLOSUM was used as 'cost matrix' with 'gap open cost': 10 and 'gap extend cost': 0.1. Phylograms were made using the neighbour-joining algorithm with the Jones–Taylor–Thornton model [26]. The bootstrapping analysis involved 200 replicates. In order to visualize the data, the Geneious 6.1.7 software was applied.

### RNA isolation, cDNA amplification and quantitative real-time PCR analysis

The RNA of the *Mo*WT and the mutants was isolated using an RNeasy Plant Mini kit (QIAGEN) following the manufacturer's instructions for purification of total RNA from plants and filamentous fungi. The cDNA amplification and quantitative real-time PCR (qPCR) were performed using the iScript One-Step RT-PCR kit with SYBR Green (Bio-Rad Laboratories) following the manufacturer's instructions. We used the constitutive expressed fungal elongation factor EF-1 alpha (MGG_03641) genes and actin (MGG_03982) as reference (housekeeping) genes for the relative quantification of the expression ratio. Calculations were based on the relative quantification calculation method of Pfaffl [27].

### Fermentation and growth conditions for secondary metabolism and quantitative real-time PCR analysis

Three agar blocks of 10 mm diameter from 11-day-old *M. oryzae* cultures were aseptically transferred as inoculum to 200 ml liquid CM in 500 ml glass flasks with one baffle. These cultures were grown for 72 h at 26 °C and 120 r.p.m. The mycelium was washed with sterile water and was transferred to different liquid starvation media, and the fermentation was then continued at 26 °C and 120 r.p.m. in an orbital shaker. The media used in this study were minimal medium (MM) [19] and rice-extract medium (REM; 10 g rice leaves of 28-day-old rice cultivar CO39 were shredded and added to 1 l MM before sterilization).

### Preparation of crude extracts from *M. oryzae* cultures

The mycelium was separated from the culture fluid by filtration. The culture fluid was extracted twice with ethyl acetate and equal amounts of the crude extracts obtained were then dried with $Na_2SO_4$. After evaporation of the organic solvent *in vacuo* at 40 °C to dryness, the residue was dissolved in methanol to give 10 mg $ml^{-1}$. The mycelium was extracted for 60 min with a methanol/acetone mixture (1 : 1, v/v). The crude extract was filtered and evaporated *in vacuo* at 40 °C to dryness and dissolved in methanol to give 10 mg $ml^{-1}$.

### Isolation of the pyriculol derivatives from cultures of *M. oryzae*

A fermenter (20 l; B. Braun) with MM was inoculated with a 5-day-old *M. oryzae* 70-15 (*Mo*WT) fluid culture (500 ml CM in a 1 l glass flask with one baffle). The culture conditions were as follows: 3 l air $min^{-1}$; 28 °C; 120 r.p.m. Fermentation was stopped when pyriculol was produced in good yields (traced by HPLC). The culture fluid was separated from the mycelium by filtration and extracted with ethyl acetate (1 : 1, v/v) to yield 280 mg crude extract. Solid-phase extraction (Chromabond $C_{18}$ 2 g; Macherey-Nagel) of the crude extract with a $H_2O$/acetonitrile gradient yielded 68 mg intermediate 1 [66 % (v/v) acetonitrile]. Intermediate 1 was subjected to a preparative separation [column: Waters Sunfire C18, 19×250 mm, 5 µm; solvents: $H_2O$/acetonitrile; isocratic flow: 27 % (v/v) acetonitrile; flow: 15 ml $min^{-1}$]. Pyriculol was isolated (28 mg) at retention time 6 min.

Furthermore, a fermenter (20 l) with BAF medium [ingredients per litre ($H_2O$): 20 g maltose, 10 g glucose, 2 g soy peptone, 1 g yeast extract, 0.5 g $KH_2PO_4$, 1 g $MgSO_4.7H_2O$, 10 mg $FeCl_3$, 1 mg $ZnSO_4.7H_2O$ and 5 ml 0.1 M $CaCl_2$] was inoculated with a 7-day-old *Mo*WT fluid culture (500 ml BAF medium in a 1 l glass flask with one baffle). The culture conditions were as follows: 3 l air $min^{-1}$; 28 °C; 130 r.p.m. Fermentation was stopped when the compounds desired were produced in good yields (traced by HPLC/MS; 7 days). The culture fluid was separated from the mycelium by filtration and extracted with ethyl acetate (1 : 1, v/v) to yield 806 mg crude extract. Solid-phase extraction (Chromabond $C_{18}$ 2 g; Macherey-Nagel) of the crude extract with a $H_2O$/acetonitrile gradient yielded 365 mg intermediate 1 [10 % (v/v) acetonitrile], 195 mg intermediate 2 [35 % (v/v) acetonitrile, containing the pyriculol derivatives] and 24 mg intermediate 3 [100 % (v/v) acetonitrile]. Intermediate 2 was subjected to a preparative separation [column: Waters Sunfire C18, 19×250 mm, 5 µm; solvents: $H_2O$/acetonitrile; gradient: 5–25 % (v/v) acetonitrile in 30 min; 25–32 % (v/v) acetonitrile in 60 min; flow: 13.6 ml $min^{-1}$]. The following pyriculol derivatives were isolated: dihydropyriculariol (1.5 mg; retention time, 26.5 min), dihydropyriculol (3.4 mg; retention time, 27–27.5 min) and pyriculariol (7.3 mg; retention time, 48.5–49 min).

### HPLC/MS method for analysis of secondary metabolites from *M. oryzae*

Crude extracts were analysed by means of HPLC (Agilent 1100 Series) equipped with a LiChrospher RP 18 (3×125 mm; 5 µm, Merck) and a diode array detector. In order to analyse the extracts, the temperature of the column was set to 40 °C and a flow rate of 1 ml $min^{-1}$ was used with an elution gradient composed of $H_2O$ and acetonitrile.

The molecular weight of the peaks selected was determined using an HPLC/MS (Agilent 1260 Series LC and 6130 Series Quadrupole MS System). The mass spectra were recorded using atmospheric pressure chemical ionization with positive and negative polarization. A Superspher RP 18 (125×2 mm; 4 µm, Merck) column was used at 40 °C. For every run, 1 µl of a sample at a concentration of 1 mg $ml^{-1}$ was injected. The elution was performed with a gradient of $H_2O$ and acetonitrile, and a flow rate of 0.45 ml $min^{-1}$.

### Identification of pyriculol, pyriculariol, dihydropyriculol and dihydropyriculariol

Isolated samples were analysed by $^1H$ NMR (600 MHz, $CDCl_3$, Bruker DRX-600 spectrometer). The NMR spectrum as well as the $^1H$ NMR data is given in supplementary material S2.

### Phytotoxicity assay with rice and plant infections/ pathogenicity assays with rice

The phytotoxicity assays were carried out using leaf segments of 21-day-old plants of dwarf indica rice cultivar CO39. Plants were cultivated using a daily cycle of 16 h light followed by 8 h darkness [28 °C, 90 % (v/v) relative humidity]. Leaves were fixed on water agar and the extracts were applied in 10 µl droplets of $H_2O$ containing 0.2 % (w/v) gelatin to a final amount of 10 µg of each extract. Pure compounds were applied in 10 µl droplets with an additional control of the solvent used. The results were documented by photography 5 days post-application. The plant infection assays were carried out as described previously [19].

## RESULTS

### Secondary metabolites produced by *M. oryzae* strain 70-15 in axenic cultures

In order to investigate the secondary metabolism of *M. oryzae* 70-15 (*Mo*WT), the fungal strain was grown under different culture conditions that affect secondary metabolite

production. Crude extracts of the submerged cultures were analysed by HPLC/MS to identify secondary metabolites produced by the rice blast fungus. Levels of four polyketides were found to be boosted in axenic cultures in MM (synthetic medium) and in REM (rice leaf extract based medium). The respective metabolites produced under these conditions were identified as the heptaketides pyriculol [2-((1*E*,5*E*)-3,4--dihydroxy-1,5-heptadienyl)-6-hydroxybenzaldehyde], pyriculariol [2-((1*E*,3*E*)-5,6-dihydroxy-1,3-heptadienyl)-6-hydro xybenzaldehyde], dihydropyriculol [2-((1*E*,5*E*)-3,4-dihydroxy-1,5-heptadienyl)-2-hydroxymethylphenol] and dihydropyriculariol [3-((1*E*,3*E*)-5,6-dihydroxy-1,3-heptadienyl)-2 -hydroxymethylphenol] (Fig. 1). The same compounds were found in the corresponding extracts of mycelia, but only in very low quantities. The highest total yield of secondary metabolites was observed in extracts of cultures grown in MM, and the best pyriculol production in REM (data not shown).

Pyriculol is a heptaketide consisting of seven $C_2$ groups, wherein of the seven $C_2$ groups within the native polyketo compound, only one aldehyde group remains in the $C_1$position (Fig. 1). The hydroxyl group at the $C_{11}$ position of pyriculol can be obtained via a single reduction step and further reductions on the $C_5$, $C_7$, $C_9$ and $C_{13}$ positions may lead to the double bonds within the molecule. Furthermore, the $C_{10}$ position of pyriculol contains a third hydroxyl moiety. Since pyriculol and its derivatives should be produced by a PKS, we searched for genes encoding such proteins in the *M. oryzae* genome. Several reduced moieties (-OH/-H) within the structure of pyriculol indicate that reductase and dehydratase domains are essential, whereas methyltransferase activity is apparently not required for the biosynthesis of heptaketides.

## Sequence analysis and identification of polyketide synthase-related genes in *M. oryzae*

Sequence analysis and comparison of the predicted protein sequences of putative PKS-encoding genes revealed a set of 20 relevant ORFs within the *M. oryzae* genome (Table S2). Selected genes were found to contain the four PKS-characteristic protein domains [PF00109 (KS-N, N-terminal $\beta$-ketoacyl synthase), PF02801 (KS-C, C-terminal $\beta$-ketoacyl synthase), PF00698 (AT, acyltransferase) and PF00550 (PP, phosphopantethin-binding sequence)]. In addition, the resulting sequences contained further significant domains: PF14765 (DH, dehydratase), PF08659 (KR, ketoreductase), PF08242 (MT, methyltransferase), PF08240/PF00107 (ADH/ADHZ, alcohol dehydrogenases) and PF00975 (TE, thioesterase). Furthermore, we also identified a set of 18 putative NRPS and PKS-NRPS hybrids (Table S3). These ORFs were found to contain additional NRPS-characteristic protein domains (PF00501: AMP, AMP-binding enzyme and PF00668: CD, condensation domain).

## Transcript level of *MoPKS19* correlates with the biosynthesis rate of pyriculol/pyriculariol

The PKS-encoding genes *MoPKS4*, *MoPKS12-MoPKS17*, *MoPKS19* and *MoPKS22* were assumed to be the most promising candidates for initial analysis. Their predicted protein sequences contain essential KR and DH domains, whereas MT domains were not found. The transcript abundance of *MoPKS19* was the most significantly affected in the experiments. *MoPKS19* transcript was increased by fivefold in REM compared to CM at 4 h after transfer to REM (Fig. 2). This increase in *MoPKS19* expression is correlated with the production of pyriculol. Expression of other PKSs was either repressed in REM compared to CM (*MoPKS4*, *MoPKS12*, *MoPKS14*, *MoPKS16*, *MoPKS17* and *MoPKS22*) or not upregulated (*MoPKS13* and *MoPKS15*). REM was selected for a time course experiment to investigate the *MoPKS19* transcript abundance in comparison to the pyriculol/pyriculariol production rate. The relative transcript abundance of *MoPKS19* increased in a time-dependent manner, similar to increasing amounts of pyriculol in corresponding extracts of the culture filtrate samples (Fig. 3). The maximal pyriculol concentration and the highest *MoPKS19* transcript abundance were observed 8 h after transfer from CM to REM. Overall, the expression pattern of *MoPKS19* in REM was found to correlate with the kinetics of pyriculol production. Additionally, the *MoPKS19* transcript abundance was analysed *in planta* during rice infection. The *MoPKS19* transcript was found to be increased during invasive growth (Fig. S1).

## Analysis of *MoPKS19* and identification of *MoPKS19*-clustered genes

The gene sequence, including the flanking areas, was analysed by genome analysis in order to get more detailed information concerning *MoPKS19*. Therefore, sequence analysis of *MoPKS19* was conducted by means of the InterProScan database and conserved domains are presented in a scheme of the protein sequence (Fig. 4b, Table 1). In addition, phylogenetic analysis of amino acid sequences of MoPks19 was conducted and is provided in Fig. S2.

Since multiple genes may participate in one biosynthetic gene cluster close together in filamentous fungi, we also analysed the genes neighbouring *MoPKS19*. A total of 30 ORFs next to *MoPKS19* were examined and their putative function with respect to secondary metabolism and the biosynthesis of pyriculol was assessed (Table 1, Fig. 4a).

It was suggested that oxidation steps or reduction steps of the heptaketides are required in order to obtain the oxidized forms pyriculol and pyriculariol, respectively the reduced compounds dihydropyriculol and dihydropyriculariol (Fig. 1). In addition to the coding sequence of the *MoPKS19* gene, two genes were identified containing conserved domains for FAD_binding (PF01565). This domain has been found to be characteristic for oxidase activity [28]. The two genes were named *MoC19OXR1* and *MoC19OXR2* (Table 1). Furthermore, three genes probably encoding reductases were located close to the *MoPKS19* gene. The three ORFs possess sequences coding for short-chain dehydrogenase/reductase domains (PF00106/PF13561; Table 1). Due to the putative role of the corresponding proteins as reductases, the encoding genes were named *MoC19RED1*,

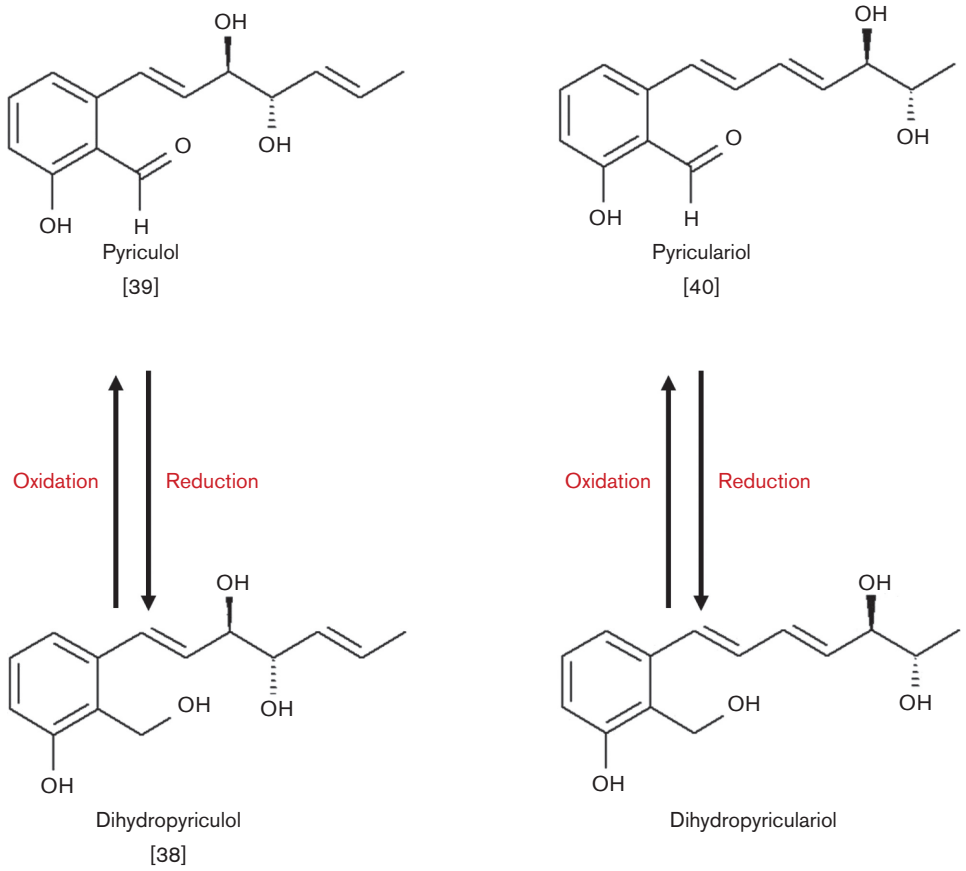


**Fig. 1.** Secondary metabolites produced by *M. oryzae* 70-15 (*Mo*WT). The structures of the major polyketides found in extracts of *Mo*WT after fermentation in MM or in REM are shown.

*MoC19RED2* and *MoC19RED3*. Since the transcriptional activation of the genes is likely to be needed for regulation of the *MoPKS19* gene, two ORFs including sequences for a homeobox domain (PF00046) and a fungal-specific transcription domain (PF04082) were analysed in detail. The genes were named *MoC19TRF1* and *MoC19TRF2* (Table 1). Gene clusters often comprise genes coding for transporters in order to export secondary metabolites. Two genes with adequate domains were identified as *MoC19ABC7* and *MoC19MFS1*. *MoABC7* has already been published in a comprehensive study of ABC transporters in *M. oryzae*, where its function was not linked to secondary metabolism [29]. Function and position of genes identified near *MoPKS19* suggest the presence of a putative cluster of secondary metabolite genes (Fig. 4a). Further studies (co-expression, deletion mutants) are needed to demonstrate the role of this putative secondary metabolite cluster in pyriculol biosynthesis.

## Inactivation of *MoPKS19* resulted in mutants deficient in heptaketide production

In order to prove that the gene product is the key enzyme in pyriculol biosynthesis, the *MoPKS19* gene was inactivated, resulting in the mutant strain Δ*Mopks19*. The HPLC chromatogram of the culture filtrate extract from *Mo*WT in comparison to extracts of the 'loss of function' mutant Δ*Mopks19* and the complemented strain Δ*Mopks19*/*MoPKS19* showed complete absence of the heptaketides in extracts of Δ*Mopks19*. Neither pyriculol nor pyriculariol nor the dihydro derivatives were detected in extracts of Δ*Mopks19*, whereas reintegration of the intact gene *MoPKS19* into the genome of Δ*Mopks19* rescued the phenotype in terms of the heptaketide biosynthesis (Fig. 5a). Thus, the secondary metabolite analysis revealed that the mutant strain Δ*Mopks19* was unable to produce pyriculol and pyriculariol, further underlining the essential role of *MoPKS19* in the biosynthesis.

Since two putative oxidase-encoding genes (*MoC19OXR1* and *MoC19OXR2*) and three reductase-encoding genes (*MoC19RED1*, *MoC19RED2* and *MoC19RED3*) were identified within the putative *MoPKS19* gene cluster (Table 1, Fig. 4a), these enzymes were of particular interest concerning their function in pyriculol biosynthesis. However, we were unable to generate inactivation mutants of *MoC19OXR2*, *MoC19RED1*, *MoC19RED2* and *MoC19RED3*. Gene inactivation, loss of

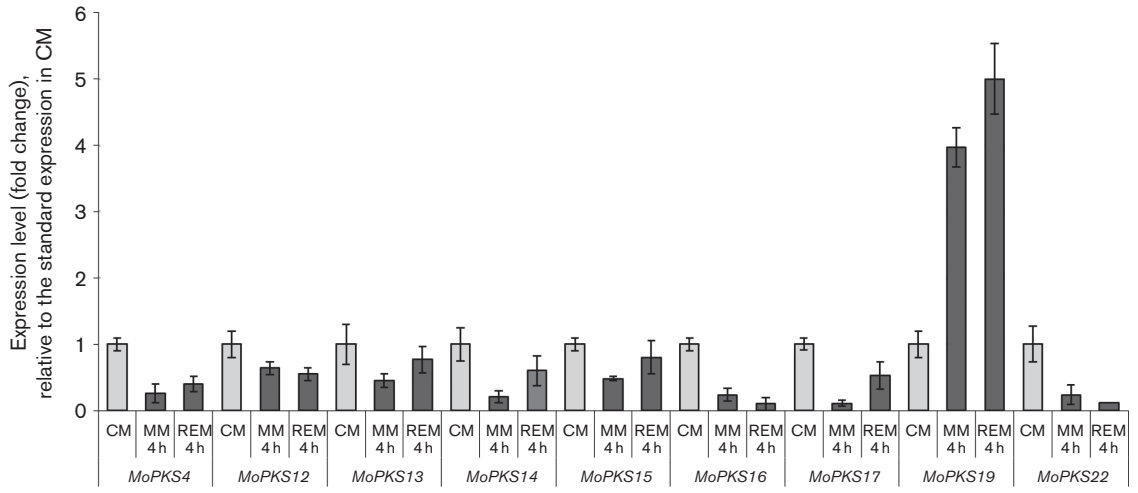


**Fig. 2.** qRT-PCR analysis of the expression level from genes encoding reducing non-methylating PKS in *Mo*WT. The *M. oryzae* cultures were grown in CM for 72 h at 26 °C and 120 r.p.m. The mycelium was then transferred to MM, REM or CM for further submersed cultivation at 26 °C and 120 r.p.m. Samples were taken after 2 and 4 h and RNA was isolated from the mycelium samples for qRT-PCR analysis. The results of transcript abundance in MM or REM are given relative to quantification in CM. The experiments were conducted in triplicate. CM, complete medium; MM, minimal medium; REM, rice-extract medium.

function andoverexpression mutants of the *MoC19OXR1* gene, could be generated. The analysis of the HPLC chromatograms of extracts frosm Δ*MoC19oxr1* and *MoEF1*::*C19OXR1* validated the putative function in pyriculol biosynthesis because the reduced dihydro compounds were detectable exclusively in the extracts of the inactivation mutant Δ*MoC19oxr1,* whereas the oxidized forms were found exclusively in the extracts of the overexpression mutant *MoEF1*::*C19OXR1* (Fig. 5a). Reintegration of the intact gene *MoC19OXR1* into the genome of Δ*MoC19oxr1* restored the phenotype of *Mo*WT (data not shown). As a conclusion, MoC19Oxr1p appears to be responsible for conversion of dihydropyriculol and dihydropyricullariol into pyriculol and pyricullariol, respectively.

## Regulators of pyriculol biosynthesis within the putative *PKS19* gene cluster

Since we were not able to inactivate the genes *MoC19RED1*, *MoC19RED2*, *MoC19RED3* and *MoC19OXR2*, it was impossible to assess the function of these genes in secondary metabolite production. We conducted quantitative PCR analysis of these oxidase/reductase genes identified within the putative *MoPKS19* gene cluster to identify enzymes responsible for the reduction of pyriculol and pyricullariol (Fig. 6a). Transcript abundance of the selected genes *MoC19RED1*, *MoC19RED2*, *MoC19RED3*, *MoC19OXR1* and *MoC19OXR2* during the growth in axenic culture in REM was found to be upregulated relative to the growth in CM (Fig. 6a). Furthermore, we checked the transcript abundance of the selected genes relative to elongation factor EF-1 alpha, which is known to have stable and high transcript levels. Solely *MoRED3* transcript abundance was found to be even higher than *MoEF1* abundance in CM, MM and REM (Fig. S3). All other genes showed lower transcript levels compared to *MoEF1*.

The regulation dynamics within the putative *PKS19* gene cluster and the contribution of the two transcription factors *MoC19TRF1* (MGG_04843) and *MoC19TRF2* (MGG_04853) to pyriculol production were also investigated. Therefore, the transcript abundance of the *MoPKS19* gene was determined in the inactivation mutants Δ*MoC19TRF1* and Δ*MoC19TRF2* and in the expression mutants *MoEF1*::*C19TRF1* and *MoEF1*::*C19TRF2*. Naturally, we initially checked the transcription of the target genes *MoC19TRF1* and *MoC19TRF2* in the generated mutant strains and found complete transcript absence in Δ*MoC19TRF1* and Δ*MoC19TRF2* whereas we observed a strong increase of transcript abundance in the overexpression strains (data not shown). The relative transcript level of *MoPKS19* was found to be increased in the inactivation mutants, either in high pyriculol producing or in low producing conditions (Figs 6b and S1). By contrast, transcript abundance of *MoPKS19* was found to be constant, at the mostslightly decreased in the overexpression mutants compared to *Mo*WT (Figs 6b and S1). These results suggest that these two transcription factors act as negative regulators of *MoPKS19*.

## Pyriculol and pyricullariol appear to induce lesion formation upon application on rice leaves but are dispensable for pathogenicity of *M. oryzae* 70-15

The crude extract of *Mo*WT containing the heptaketides induced lesion or 'green isle' formation on host plant leaves, whereas no disease symptoms were observed after exposure of leaf segments to extracts of Δ*Mopks19* and Δ*MoC19oxr1* containing no pyriculol, oronly the reduced dihydro derivatives (Fig. 5a). Pyriculol and pyricullariol appear to be essential for lesion-inducing effects on rice plants, while the dihydro derivatives appear to be inactive in that respect.

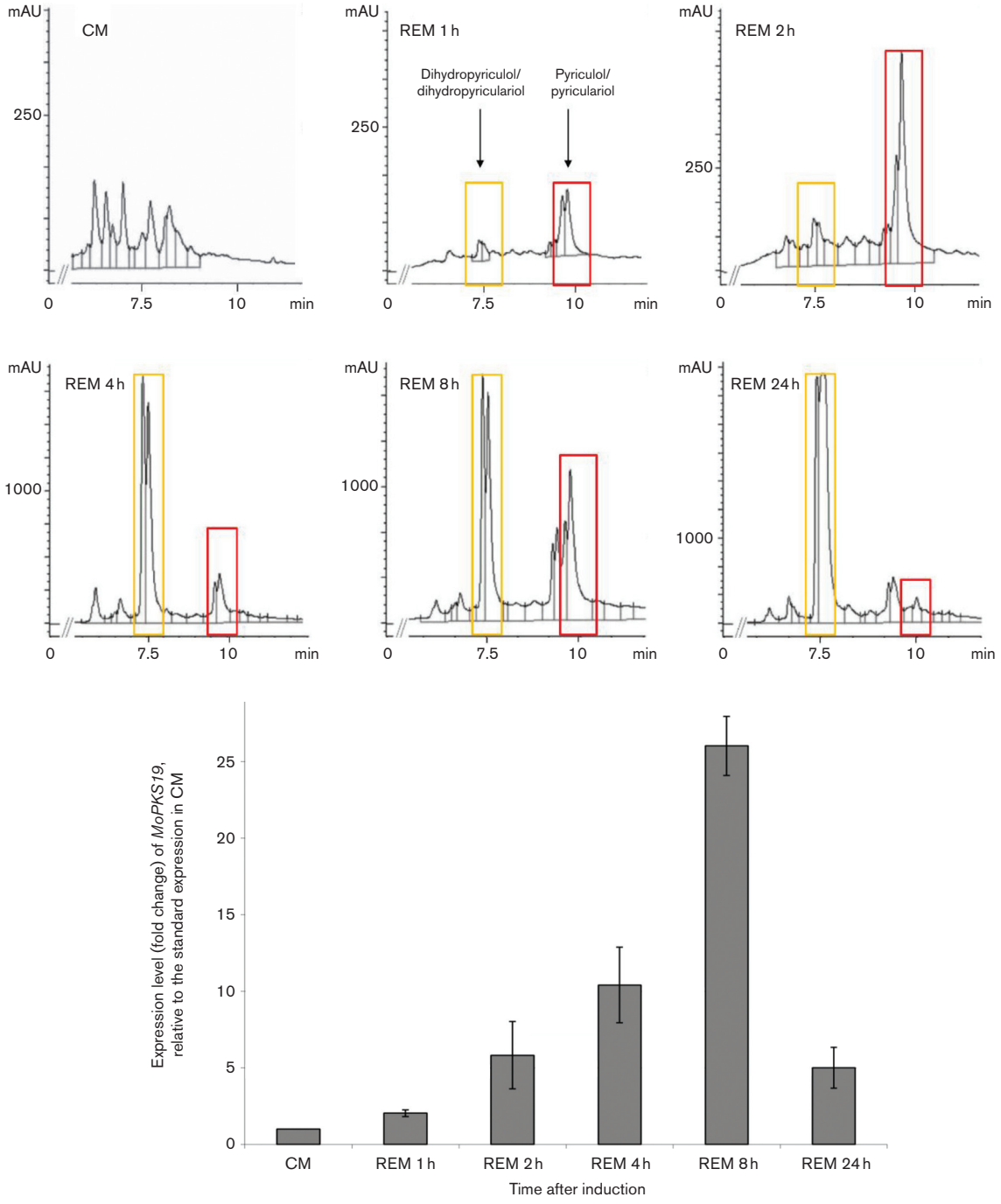


**Fig. 3.** Time-dependent HPLC analysis of culture filtrate extracts from *Mo*WT in correlation to qRT-PCR analysis of the expression level from the *MoPKS19* gene. The *M. oryzae* cultures were grown as described in Methods. Samples were taken 1, 2, 4, 8 and 24 h after transfer to REM. The HPLC analysis was conducted using extracts of the culture broth, and RNA was isolated from the mycelium samples. The results of transcript abundance in REM are given relative to quantification in CM. The experiments were conducted in triplicate. CM, complete medium; REM, rice-extract medium; mAU, milli-absorption units. Bars represent (+/−) SEM.

Furthermore, qRT-PCR results showed a slightly increase of *MoPKS19* transcript abundance *in planta* during infection (Fig. S1). Complementation experiments with reintegration of the intact gene *MoPKS19* into the genome of Δ*Mopks19* and *MoC19OXR1* into the genome of Δ*MoC19oxr1* rescued the phenotype in terms of phytotoxicity and the results were comparable to wild-type extracts. The assays were conducted with the pure compounds isolated from the extracts

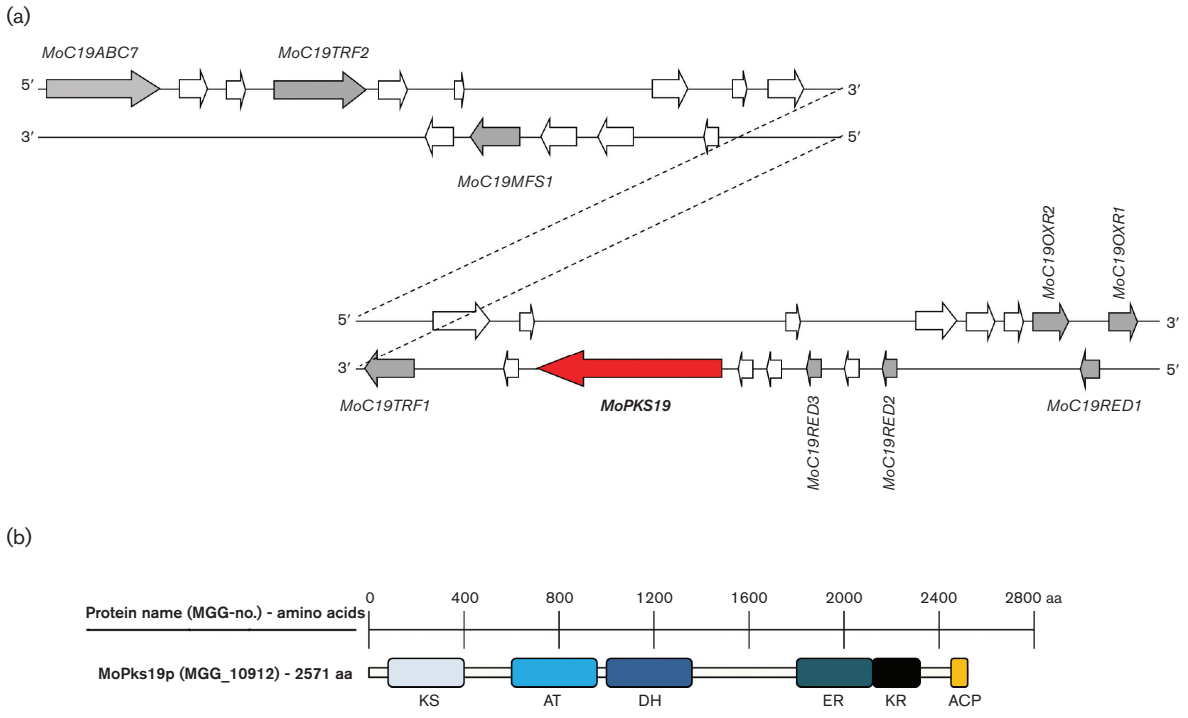


**Fig. 4.** Schematic presentation of the *MoPKS19* gene cluster in the genome of *Mo*WT. (a) A scheme of 30 ORFs neighbouring the *MoPKS19* gene is presented. The genes are shown with their position either on the 'sense (5′–3′)' or on the 'antisense (3′–5′)' strand. White arrows imply genes with no obvious functions with significant use in this study (e.g. hypothetical proteins without predicted protein domains). (b) Schematic presentation of protein domains of MoPks19p. KS, $\beta$-Ketoacyl synthase; AT, acyltransferase; DH, dehydratase; ER, enoyl reductase; KR, ketoreductase; ACP, ACP domain.

of *M. oryzae* cultures in order to provide evidence for pyriculol and pyriculariol being responsible for the phytotoxic effects. Pyriculol and pyriculariol induced the 'green isles', whereas the dihydro compounds were not found to be phytotoxic (Fig. 5b). Furthermore, the same assays were carried out on leaf segments of wheat and barley and revealed comparable results (data not shown).

Rice plants were infected with conidia of *Mo*WT and the mutant strains Δ*Mopks19*, Δ*MoC19oxr1*, *MoEF1*::*C19OXR1*, Δ*MoC19TRF1*, Δ*MoC19TRF2*, *MoEF1*::*C19TRF1* and *MoEF1*::*C19TRF2* in order to further assess whether pyriculol or pyriculariol is of relevance for pathogenicity or virulence in the rice blast fungus. The numbers of lesions found on plants treated with conidia of the *Mo*WT and the respective mutant strains were equal (Fig. S4). Thus, loss of pyriculol biosynthesis did not affect the pathogenicity in *M. oryzae*.

## DISCUSSION

Toxins produced by the pathogen were found to be important virulence factors in many fungal plant diseases [30]. The secondary metabolite spectrum of the hemibiotrophic fungus *Mo*WT includes among others the polyketide pyriculol, its isomer pyriculariol and reduced dihydro derivatives of both compounds (Fig. 1). Further secondary metabolites previously described to be produced by the rice blast fungus, for example, pyrichalasin H [31], pyriculol [32] or tenuazonic acid [12–14], were not found in this study. Based on considerations concerning the chemical structure of pyriculol, we searched for PKS-encoding genes in the genome of *M. oryzae*. The pyriculol molecule contains several hydroxyl moieties and double bonds, so it can be assumed that reduction steps occurred during biosynthesis. This reaction could be executed by a PKS itself or partly by tailoring enzymes [33]. The variety of PKS-related genes was, consequently, restricted to genes containing a conserved ketoreductase domain (PF08659). Moreover, pyriculol is composed of a linear polyketide chain of seven $C_2$ units without any branch. Subsequent methylation could not been hypothesized since the biosynthetic process of polyketide methylation followed by demethylation has never been observed in fungi [34] and, subsequently, the number of candidate genes involved in pyriculol biosynthesis was further reduced to those without a methyltransferase domain (PF08242). The qRT-PCR analysis of the remaining nine putative PKS-encoding genes resulted in a high transcript abundance of *MoPKS19* (Fig. 2). The detailed sequence analysis of *MoPKS19* resulted in significantly conserved protein domains (Fig. 4b). With these conserved domains, MoPks19p should be able to synthesize a polyketide such as pyriculol and implement the two reduction steps to the

**Table 1.** Neighbouring genes to *MoPKS19* within the *Mo*WT genome with putative function of the corresponding proteins

The MGG numbers of the genes neighbouring *MoPKS19* (30 ORFs) of the eighth annotation of the *M. oryzae* genome are listed. The InterPro search of conserved protein domains resulted in information concerning the putative protein function.

| MGG–no. | Gene name | Protein size (aa) | Protein domains (InterPro) | Putative function |
|---|---|---|---|---|
| MGG_04855 | ***MoC19ABC7*** | 1683 | ABC_membrane (PF00664)<br>ABC_trans (PF00005) | Membrane transport |
| MGG_04854 | Hyp. prot | 394 | Adaptin-binding (PF10199) | – |
| MGG_16817 | Hyp. prot | 81 | – | – |
| MGG_04853 | ***MoC19TRF2*** | 625 | Homeobox (PF00046) | Transcription factor |
| MGG_04852 | – | 1279 | E1-E2_ATPase (PF00122)<br>HAD (PF12710) | Membrane ATPase |
| MGG_04851 | Hyp. prot | 392 | – | – |
| MGG_16816 | Hyp. prot | 57 | – | – |
| MGG_04850 | ***MoC19MFS1*** | 616 | MFS_1 (PF07690) | Membrane transport |
| MGG_12978 | – | 505 | FAD_binding_3 (PF01494) | Monooxygenase |
| MGG_12979 | Hyp. prot | 545 | – | – |
| MGG_04847 | – | 449 | Peptidase_M14 (PF00246) | Carboxypeptidase |
| MGG_04846 | Hyp. prot | 198 | – | – |
| MGG_04845 | – | 246 | – | – |
| MGG_04844 | Hyp. prot | 512 | – | – |
| MGG_04843 | ***MoC19TRF1*** | 610 | Fungal_trans (PF04082) | Transcription factor |
| MGG_04842 | – | 776 | Aconitase (PF00330) | Isomerization reaction |
| MGG_04841 | Hyp. prot | 241 | – | |
| MGG_16815 | Hyp. prot | 210 | – | – |
| MGG_10912 | ***MoPKS19*** | 2571 | KS (PF00109)<br>AT (PF00698)<br>DH (PF14765)<br>ER (IPR020843)<br>KR (PF08659)<br>ACP (IPR009081) | Polyketide synthase |
| MGG_10911 | – | 198 | Cupin_2(PF07883) | Storage protein |
| MGG_15115 | Hyp. prot | 104 | – | – |
| MGG_16814 | Hyp. prot | 81 | – | – |
| MGG_10910 | ***MoC19RED3*** | 250 | adh_short (PF00106) | Dehydrogenase/reductase |
| MGG_12981 | – | 205 | Cupin_2 (PF07883) | Storage protein |
| MGG_12982 | ***MoC19RED2*** | 278 | adh_short_C2 (PF13561) | Dehydrogenase/reductase |
| MGG_15114 | Hyp. prot | 458 | FAD_binding_3 (PF01494) | Monooxygenase |
| MGG_16813 | Hyp. prot | 363 | Aldo_ket_red (PF00248) | – |
| MGG_16812 | ***MoC19OXR2*** | 520 | FAD_binding_4 (PF01565)<br>BBE (PF08031) | Oxidase |
| MGG_12983 | ***MoC19RED1*** | 284 | adh_short (PF00106) | Dehydrogenase/reductase |
| MGG_10961 | ***MoC19OXR1*** | 507 | FAD_binding_4 (PF01565)<br>BBE (PF08031) | Oxidase |

double bonds. Nine genes likely involved in secondary metabolism were identified near *MoPKS19* (Fig. 4a). Three reductases, two oxidases, two putative transcription factors and two membrane transporters were located close to *MoPKS19* in the genome (Table 1; Fig. 4a). We identified that *MoPKS19* is involved in pyriculol synthesis and *MoC19OXR1*, as an oxidase gene, is involved in the biosynthetic pathway. The two transcription factors *MoC19TRF1* and *MoC19TRF2* appear to act as negative regulators of *MoPKS19*, since the transcript level of *MoPKS19* in the loss of function mutants was found to be increased (Fig. 6b). There was no need to compare the expression pattern of *MoC19OXR1*, *MoC19TRF1* and *MoC19TRF2* to *MoPKS19* in this study because transcript abundance must not correlate with protein function. The extracts of the mutant strain Δ*Mopks19* did not contain heptaketides, the oxidized forms pyriculol/pyriculariol or the reduced dihydro derivatives (Fig. 5a). qRT-PCR analysis showed a strong correlation of *MoPKS19* transcript abundance with pyriculol production (Fig. 3) suggesting the essential role of *MoPKS19* in pyriculol/pyriculariol production. Modifications of the heptaketide-like conversions from the oxidized molecules into the reduced dihydro derivatives and *vice versa* can be accomplished from the remaining enzymes coded in the putative

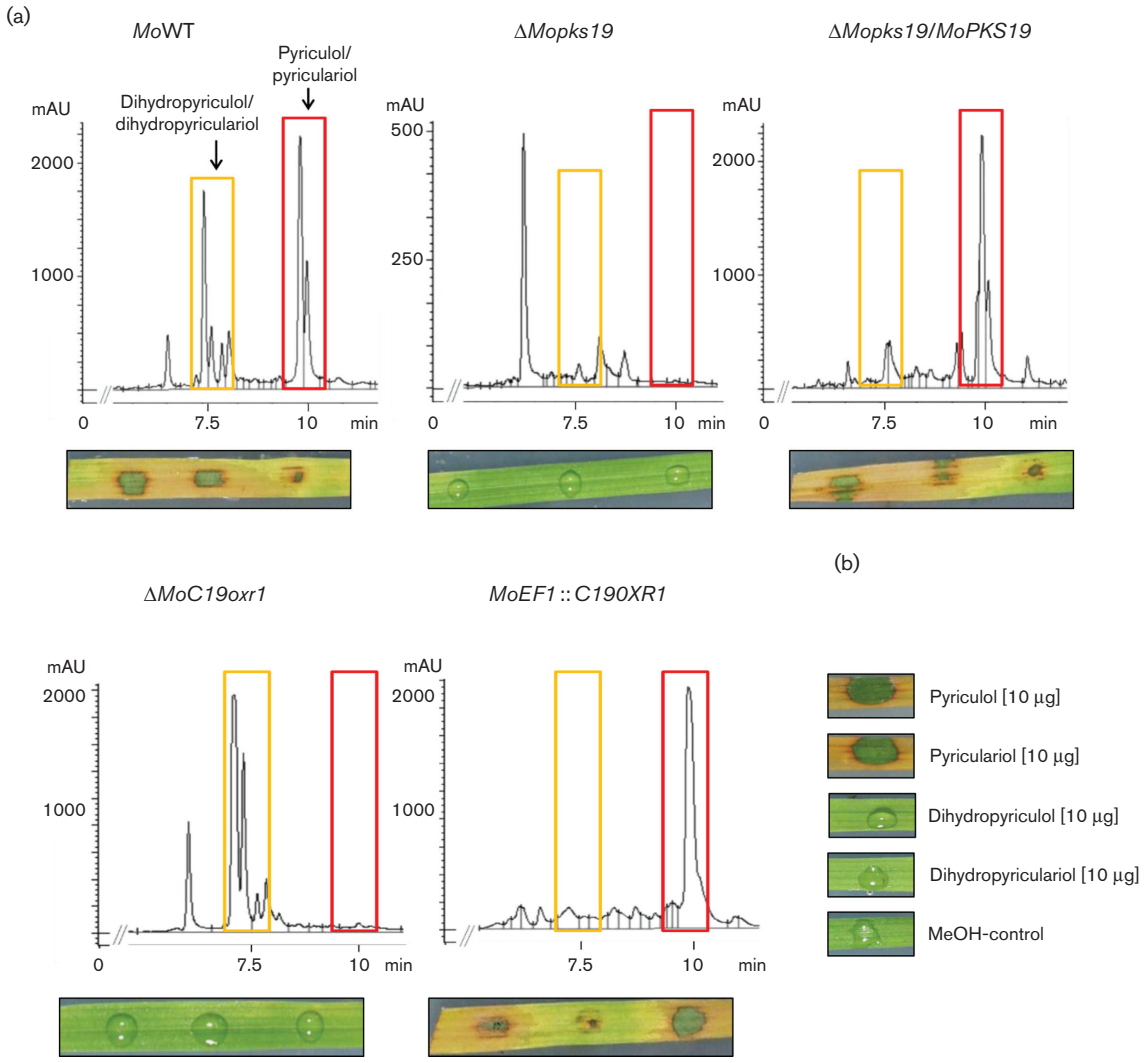


**Fig. 5.** Analysis of polyketide in culture filtrate extracts from *M. oryzae* and phytotoxic activity of extracts and pure compounds. (a) HPLC chromatograms of extracts from *Mo*WT, Δ*Mopks19*, Δ*Mopks19/MoPKS19*, Δ*MoC19oxr1* and the overexpression mutant *MoEF1*::*C19OXR1*. The *M. oryzae* cultures were grown as described in Methods. Samples were taken 8 h after transfer to REM. The HPLC analysis was conducted using extracts of the culture broth (210 nm wavelength). mAU, Milli-absorption units. Phytotoxic activity of the extracts towards rice leaves is shown below each chromatogram. The assays were conducted as described in Methods. (b) Phytotoxicity was monitored for the pure compounds under equal conditions.

*MoPKS19* cluster (Table 1; Fig. 4a). In this context, we identified *MoC19OXR1* as essential for pyriculol synthesis, since the mutant strain Δ*MoC19oxr1* was not able to produce the oxidized molecules pyriculol and pyriculariol, but rather the reduced dihydro compounds. By contrast, overexpression of *MoC19OXR1* resulted in a mutant strain producing the oxidized molecules pyriculol/pyriculariol exclusively (Fig. 5a). Since fungal PKSs are known to use $C_2$, $C_3$ or $C_4$ starter molecules [35], and heptaketides, such as rubrofusarin from *Fusarium graminearum* [36] or naphthopyran and isocoumarin from *Aspergillus nidulans* [37], were built from acetyl-CoA and malonyl-CoA, the biosynthetic pathway of pyriculol may proceed in an equivalent manner. The recently proposed biosynthesis process describes pyriculol as the intermediate product and the dihydro derivatives need the pyriculol molecule as a precursor [18]. That hypothesis could be underpinned with the results in our study concerning the correlation of heptaketide synthesis and *MoPKS19* gene expression in axenic cultures of *M. oryzae*. Analysis of pyriculol production kinetics in REM showed that it is formed before its dihydro derivative (Fig. 3). In addition, we showed that only dihydro derivatives were found in extracts of Δ*MoC19oxr1* (Fig. 5a). That could be furthermore underpinned with the results of the extremely high transcript levels of *MoC19RED3* even in CM and still higher in REM (Figs 6a and S3). The pyriculol

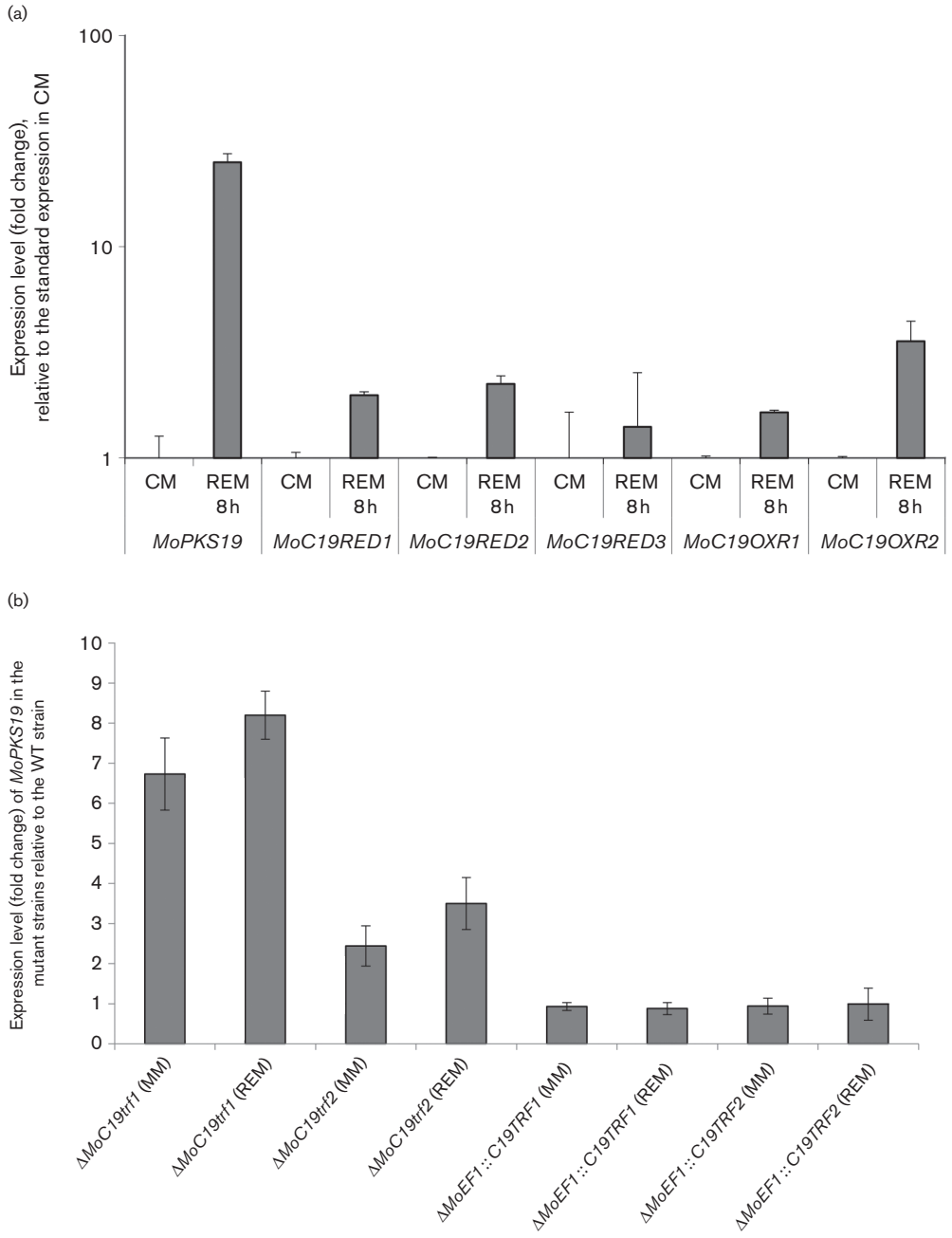


**Fig. 6.** (a) qRT-PCR analysis of the expression level from the oxidase/reductase-encoding genes in the putative *MoPKS19* gene cluster. The *M. oryzae* cultures were grown for 72 h in CM at 26 °C and 120 r.p.m. The mycelium was transferred for further submersed cultivation to REM at 26 °C and 120 r.p.m. Samples were taken before (CM control) and 8 h after the transfer to REM. The results of transcript abundance are given relative to quantification of the *MoEF1* gene in the *Mo*WT. Three replicates were made of each. (b) qRT-PCR analysis of the expression level from the *MoPKS19* gene in the mutant strains. The *M. oryzae* cultures were grown for 72 h in CM at 26 °C and 120 r.p.m. The mycelium was transferred for further submersed cultivation to MM or REM at 26 °C and 120 r.p.m. Samples were taken after 8 h. The RNA was isolated from the mycelium samples and the results of transcript abundance in REM are given relative to quantification in the *Mo*WT. Three replicates were made of each. Bars represent (+/−) SEM.

precursor molecule may be reduced to the dihydro form immediately after production. In contrast to that hypothesis, it was found that neither pyriculol nor pyriculariol but rather the dihydro forms were found in extracts of the mutant strain Δ*MoC19oxr1*, whereas pyriculol/pyriculariol could be identified exclusively in extracts of the overexpression mutant *MoEF1*::*C19OXR1* (Fig. 5a). That indicates that the dihydro derivatives may be precursors and, finally,

might be oxidized by MoC19Oxr1p to become pyriculol/pyriculariol. Overexpression of *MoC19OXR1* resulted in a mutant strain in which maybe the reductase activity of MoC19Red3p is dominated by the oxidase activity of MoC19Oxr1p. Consequently, only oxidized heptaketides were found (Fig. 5a). The dihydro derivatives of the heptaketides have been described previously as biologically inactive and not phytotoxic [38]. These findings were confirmed in our study because extracts in which only the dihydro derivatives and the pure dihydro compounds were detected failed to induce lesion formation on rice leaves (Fig. 5a, b). By contrast, extracts containing pyriculol and pyriculariol induced lesion and 'green isles' formation. Since the extracts of the Δ*Mopks19* and Δ*MoC19oxr1* mutant strains failed to induce phytotoxic lesions on rice leaves, the heptaketides can be assumed to be the sole lesion-inducing compound produced by *Mo*WT under the culture conditions applied within the present study. As a consequence, pyriculol and pyriculariol do not appear to be virulence factors in *M. oryzae*, since the mutant strains Δ*Mopks19* and Δ*MoC19oxr1* were found to be as virulent as the *Mo*WT strain, whereas these mutant strains have lost the capacity to make the lesion-inducing constituents (Figs 5a, b and S4). This conclusion gives rise to the question why a pathogen wastes energy to produce a lesion-inducing secondary metabolite if the phytotoxin is not required for disease development? Since we found increased *MoPKS19* expression levels *in planta* during invasive growth (Fig. S1), it might be possible that pyriculol can be detoxified by the plant in lower concentrations. The concentrations of the heptaketide in the extracts applied in the phytotoxicity assays resulted in phytotoxic effects maybe because of excessive compound concentrations. We have not yet been able to detect either pyriculol or the derivatives in infected rice plants and the mechanisms of induction of pyriculol synthesis are still unknown. However, the results obtained in this study concerning the molecular basis and the dynamics of regulation of the putative *MoPKS19* gene cluster give insights into the biosynthesis of the phytotoxic secondary metabolites pyriculol and pyriculariol. The identification of the genes *MoPKS19*, *MoC19OXR1*, *MoC19TRF1* and *MoC19TRF2* and their contribution to heptaketide production are reported for the first time to our knowledge and will promote further investigations concerning secondary metabolism in the rice blast fungus.

Funding information
Funding was supported by DFG SFB1212: 'Mikrobielle Umprogrammierung der Pflanzenzell-Entwicklung' and by 'Ministerium für Bildung, Wissenschaft, Weiterbildung und Kultur RLP'.

Conflicts of interest
The authors declare that there are no conflicts of interest.

References

1. Horbach R, Navarro-Quesada AR, Knogge W, Deising HB. When and how to kill a plant cell: infection strategies of plant pathogenic fungi. *J Plant Physiol* 2011;168:51–62.
2. Dean R, van Kan JA, Pretorius ZA, Hammond-Kosack KE, di Pietro A *et al.* The top 10 fungal pathogens in molecular plant pathology. *Mol Plant Pathol* 2012;13:414–430.
3. Yan X, Talbot NJ. Investigating the cell biology of plant infection by the rice blast fungus *Magnaporthe oryzae*. *Curr Opin Microbiol* 2016;34:147–153.
4. Thines E. MAP kinase and protein kinase A-dependent mobilization of triacylglycerol and glycogen during appressorium turgor generation by *Magnaporthe grisea*. *Plant Cell* 2000;12:1703–1718.
5. Langfelder K, Streibel M, Jahn B, Haase G, Brakhage AA. Biosynthesis of fungal melanins and their importance for human pathogenic fungi. *Fungal Genet Biol* 2003;38:143–158.
6. Howard RJ, Ferrari MA. Role of melanin in appressorium function. *Exp Mycol* 1989;13:403–418.
7. Collemare J, Billard A, Böhnert HU, Lebrun MH. Biosynthesis of secondary metabolites in the rice blast fungus *Magnaporthe grisea*: the role of hybrid PKS-NRPS in pathogenicity. *Mycol Res* 2008;112:207–215.
8. Song Z, Bakeer W, Marshall JW, Yakasai AA, Khalid RM *et al.* Heterologous expression of the avirulence gene *ACE1* from the fungal rice pathogen *Magnaporthe oryzae*. *Chem Sci* 2015;6:4837–4845.
9. Nukina M. The blast disease fungi and their metabolic products. *J Pestic Sci* 1999;24:293–298.
10. Tsurushima T, Minami Y, Miyagawa H, Nakayashiki H, Tosa Y *et al.* Induction of chlorosis, ROS generation and cell death by a toxin isolated from *Pyricularia oryzae*. *Biosci Biotechnol Biochem* 2010;74:2220–2225.
11. Tsurushima T, don LD, Kawashima K, Murakami J, Nakayashiki H *et al.* Pyrichalasin H production and pathogenicity of *Digitaria*-specific isolates of *Pyricularia grisea*. *Mol Plant Pathol* 2005;6:605–613.
12. Umetsu N, Kaji J, Tamari K. Investigation on the toxin production by several blast fungus strains and isolation of tenuazonic acid as a novel toxin. *Agric Biol Chem* 1972;36:859–866.
13. Lebrun MH, Dutfoy F, Gaudemer F, Kunesch G, Gaudemer A. Detection and quantification of the fungal phytotoxin tenuazonic acid produced by *Pyricularia oryzae*. *Phytochemistry* 1990;29:3777–3783.
14. Yun CS, Motoyama T, Osada H. Biosynthesis of the mycotoxin tenuazonic acid by a fungal NRPS-PKS hybrid enzyme. *Nat Commun* 2015;6:8758.
15. Hof C, Eisfeld K, Welzel K, Antelo L, Foster AJ *et al.* Ferricrocin synthesis in *Magnaporthe grisea* and its role in pathogenicity in rice. *Mol Plant Pathol* 2007;8:163–172.
16. Patkar RN, Xue YK, Shui G, Wenk MR, Naqvi NI. Abc3-mediated efflux of an endogenous digoxin-like steroidal glycoside by *Magnaporthe oryzae* is necessary for host invasion during blast disease. *PLoS Pathog* 2012;8:e1002888.
17. Parker D, Beckmann M, Zubair H, Enot DP, Caracuel-Rios Z *et al.* Metabolomic analysis reveals a common pattern of metabolic reprogramming during invasion of three host plant species by *Magnaporthe grisea*. *Plant J* 2009;59:723–737.
18. Tanaka K, Sasaki A, Cao H-Q, Yamada T, Igarashi M *et al.* Synthesis and biotransformation of plausible biosynthetic intermediates of salicylaldehyde-type phytotoxins of rice blast fungus, *Magnaporthe grisea*. *European J Org Chem* 2011;2011:6276–6280.
19. Jacob S, Foster AJ, Yemelin A, Thines E. Histidine kinases mediate differentiation, stress response, and pathogenicity in *Magnaporthe oryzae*. *MicrobiologyOpen* 2014;3:668–687.
20. Green MR, Sambrook J. *Molecular cloning: a laboratory manual*, 4th ed. Cold Spring Harbor, NY: Cold Spring Harbor laboratory; 2012.
21. Odenbach D, Breth B, Thines E, Weber RW, Anke H *et al.* The transcription factor Con7p is a central regulator of infection-related morphogenesis in the rice blast fungus *Magnaporthe grisea*. *Mol Microbiol* 2007;64:293–307.

22. **Jacob S, Foster AJ, Yemelin A, Thines E.** High osmolarity glycerol (HOG) signalling in *Magnaporthe oryzae*: identification of MoYPD1 and its role in osmoregulation, fungicide action, and pathogenicity. *Fungal Biol* 2015;119: 580–594.
23. **Kramer B, Thines E, Foster AJ.** MAP kinase signalling pathway components and targets conserved between the distantly related plant pathogenic fungi *Mycosphaerella graminicola* and *Magnaporthe grisea*. *Fungal Genet Biol* 2009;46:667–681.
24. **Tamura K, Peterson D, Peterson N, Stecher G, Nei M *et al.*** MEGA5: molecular evolutionary genetics analysis using maximum likelihood, evolutionary distance, and maximum parsimony methods. *Mol Biol Evol* 2011;28:2731–2739.
25. **Larkin MA, Blackshields G, Brown NP, Chenna R, Mcgettigan PA *et al.*** Clustal W and clustal X version 2.0. *Bioinformatics* 2007;23: 2947–2948.
26. **Saitou N, Nei M.** The neighbor-joining method: a new method for reconstructing phylogenetic trees. *Mol Biol Evol* 1987;4:406–425.
27. **Pfaffl MW.** A new mathematical model for relative quantification in real-time RT-PCR. *Nucleic Acids Res* 2001;29:e45.
28. **Mattevi A, Fraaije MW, Mozzarelli A, Olivi L, Coda A *et al.*** Crystal structures and inhibitor binding in the octameric flavoenzyme vanillyl-alcohol oxidase: the shape of the active-site cavity controls substrate specificity. *Structure* 1997;5:907–920.
29. **Kim Y, Park SY, Kim D, Choi J, Lee YH *et al.*** Genome-scale analysis of ABC transporter genes and characterization of the ABCC type transporter genes in *Magnaporthe oryzae*. *Genomics* 2013; 101:354–361.
30. **Markham JE, Hille J.** Host-selective toxins as agents of cell death in plant–fungus interactions. *Mol Plant Pathol* 2001;2:229–239.
31. **Nukina M, Namai T.** Productivity of pyrichalasin H, a phytotoxic metabolite, from different isolates of *Pyricularia grisea* and from other isolates of *Pyricularia* spp. *Agric Biol Chem* 1991;55:1899–1900.
32. **Kim JC, Min JY, Kim HT, Cho KY, Yu SH.** Pyricuol, a new phytotoxin from *Magnaporthe grisea*. *Biosci Biotechnol Biochem* 1998;62: 173–174.
33. **Fischbach MA, Walsh CT.** Assembly-line enzymology for polyketide and nonribosomal peptide antibiotics: logic, machinery, and mechanisms. *Chem Rev* 2006;106:3468–3496.
34. **Baker SE, Kroken S, Inderbitzin P, Asvarak T, Li B-Y *et al.*** Two polyketide synthase-encoding genes are required for biosynthesis of the polyketide virulence factor, T-toxin, by *Cochliobolus heterostrophus*. *Mol Plant Microbe Interact* 2006;19:139–149.
35. **Khosla C, Gokhale RS, Jacobsen JR, Cane DE.** Tolerance and specificity of polyketide synthases. *Annu Rev Biochem* 1999;68: 219–253.
36. **Frandsen RJ, Nielsen NJ, Maolanon N, Sørensen JC, Olsson S *et al.*** The biosynthetic pathway for aurofusarin in *Fusarium graminearum* reveals a close link between the naphthoquinones and naphthopyrones. *Mol Microbiol* 2006;61:1069–1080.
37. **Fujii I, Watanabe A, Sankawa U, Ebizuka Y.** Identification of Claisen cyclase domain in fungal polyketide synthase WA, a naphthopyrone synthase of *Aspergillus nidulans*. *Chem Biol* 2001;8:189–197.
38. **Iwasaki S, Muro H, Sasaki K, Nozoe S, Okuda S *et al.*** Isolations of phytotoxic substances produced by *Pyricularia oryzae* Cavara. *Tetrahedron Lett* 1973;14:3537–3542.
39. **Manabu N, Takeshi S, Michimasa I, Takeshi U, Hisao T.** Pyriculariol, a new phytotoxic metabolite of *Pyricularia oryzae* cavara. *Agric Biol Chem* 1981;45:2161–2162.
40. **Iwasaki S, Nozoe S, Okuda S, Sato Z, Kozaka T.** Isolation and structural elucidation of a phytotoxic substance produced by *Pyricularia oryzae Cavara*. *Tetrahedron Lett* 1969;10:3977–3980.


Edited by: A. Alastruey-Izquierdo and V. J. Cid